DOI: 10.64302/joshusc.v31n1c.1311

PLASMON-POLAR PHONON COUPLED MODES IN InAs DIODE STRUCTURE

Le Thi Ngoc Bao[1], Le Thi Dieu Hien[1], and Dinh Nhu Thao[2]*

[1]Hue University of Sciences, Hue University

[2] Hue University of Education, Hue University

*Email: dnthao@hueuni.edu.vn; ltnbao@husc.edu.vn

Received: 3/10/2025; Received in revised form: 19/10/2025; Accepted: 21/10/2025

ABSTRACT

In this paper, results from a numerical study on characteristics of plasmon-polar phonon coupled modes in InAs p-i-n diode structure are presented. A superposition phenomenon of two new modes in frequency spectra of built-in electric field was observed when plasmon-polar phonon interaction was taken into account. Besides, a dependence of modes frequencies on carrier density is found to be similar to dispersion relations of bulk plasmon-polar phonon coupled modes. Consequently, these two new modes can be acknowledged as plasmon-polar phonon coupled modes in diode structure. Furthermore, replicated small amplitude modes due to clipping by diode structure are also found.

Keywords: InAs, p-i-n diode structure, plasmon-polar phonon interaction, coupled mode, terahertz frequency.

1. INTRODUCTION

Terahertz (THz) radiations have attracted much attention due to their potential applications such as imaging and spectroscopy [1, 2]. However, due to high costs of the current THz devices, it is imperative to find cheap THz radiation sources for more popular applications. THz radiations from surfaces of semiconductor nanostructures excited by ultrashort laser pulses promise to be potential solid-state THz sources [3-9]. When semiconductor surfaces are illuminated by ultrashort laser pulses then ultrafast charge transport, coherent optical phonons and coherent collective oscillation may appear altogether and lead to transient THz emissions [4-6]. Furthermore, in systems in which there are simultaneous plasmons and longitudinal optical (LO) phonons, there would exist interaction among them resulting in their coupled modes [10]. The existence

of coupled modes would affect the properties of such systems. Therefore, it is necessary to study characteristics of coupled modes.

InAs p-i-n diode structure could be a promising THz source due to both ultrafast acceleration of carriers and plasma oscillation. Recently, InAs has been studied extensively due to the fact that it has small effective masses of electrons and holes [11, 12], resulting in ultrafast carrier dynamics. InAs has also been reported to generate THz waves whose radiation intensity is an order higher than those of wide band-gap semiconductors such as InP and GaAs under similar experimental conditions [13].

Among many theoretical approaches, self-consistent ensemble Monte-Carlo (EMC) method is a decent choice for studies of semiconductor devices with high accuracy and stability, although it is merely a semi-classical approach [14, 15]. This semi-classical method is especially suitable for investigating submicron devices [16a, 20-22], compared with high-accuracy but very time-consuming methods such as Green's function [14], or low-accuracy but fast-computing methods such as drift-diffusion model [16a]. Besides, this EMC method has been effectively utilized to explore THz radiation emitted from nanostructures [17-19, 22-24].

In this research, plasmon-polar phonon coupled modes in InAs p-i-n diode structure was studied with an adapted Monte Carlo method [16a, 17]. Five different scatterings were used including impurities, acoustic phonons, non-polar and polar optical phonons, and plasmons scatterings. Time evolution of carrier distribution [25] is assumed following profile of laser pulses to thoroughly update ultrafast carrier dynamics at initial stage after excitation. It is assumed that a usual 3-valley model of hyperbolic dispersion relations is applied for conduction band. Double-mode phenomenon in frequency spectra of built-in electric field was observed. Moreover, bulk-like dispersion relations of these modes were found. Therefore, these two modes are thought to be plasmon-polar phonon coupled modes in diode structure. Replicas of small amplitude modes due to clipping by diode structure were also found.

The main content of the paper is organized as follows: sections 2 and 3 describes model and numerical analysis, together with findings and discussion; and section 4 presents conclusive remarks.

2. MODEL AND METHOD OF CALCULATION

The following is a description of a model of InAs p-i-n diode structure. The p-i-n diode structure are assumed to contain *p*-type and *n*-type layers connecting by an intrinsic (*i*)-layer as in Fig. 1 with the thickness of d_p, d_n, and d_i, respectively [9]. There are some origins of carriers inside the diode structure. There is a small number of intrinsic carriers from intrinsic layer and also a small amount of doped carriers from *p*-

type and *n*-type layers. Moreover, there is a majority of photoexcited carriers when diode structures are irradiated by laser pulses. The carrier distributions, as well as all other parameters, are initialized at the beginning of simulation according to model setup [26].

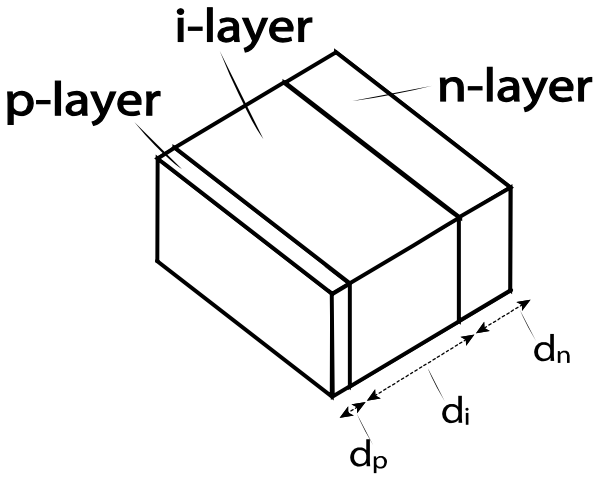

Fig. 1. Model of InAs p-i-n diode structure.

In our study, plasmon-polar phonon coupled modes in InAs p-i-n diode structures (or diodes) is investigated through built-in electric field. The built-in field is induced by all electric charges in a device, including free carriers as well as positive and negative ions. The biased field is considered as an external field so it must be set to zero. When there is a small amount of intrinsic and doped particles, oscillation of built-in electric field mainly comes from collective oscillations of photoexcited carriers. The wave-shape of built-in electric field is expected to be significantly affected by plasmon-polar phonon interaction if it exists. Therefore, characteristics of coupled modes can be revealed through analyzing built-in electric field and its Fourier transform. Fourier transform is found by fast Fourier transform algorithm integrated with a moving average filter to remove random noise of time domain signals and Hamming window filter to improve interpretation of frequency spectrum [27a].

The plasmon-polar phonon interaction leads to coupling between their modes when their frequencies are close to each other. That coupling is an interesting phenomenon that is described through a crossover behavior of curvature mode frequency versus carrier density. When the coupling exists, it is likely to see the appearance of two new modes, namely, coupled modes with their frequencies calculated as [10]

$$\omega_{\pm}^2 = \frac{1}{2}\left[(\omega_p^2 + \omega_{LO}^2) \pm \sqrt{(\omega_p^2 + \omega_{LO}^2)^2 - 4\omega_{TO}^2\omega_p^2}\right], \quad (1)$$

Where ω_{LO} and ω_{TO} are LO and transverse optical (TO) phonon frequencies and ω_p is plasma frequency [16b]

$$\omega_p = \sqrt{\frac{N_{ext} e^2}{\mu \varepsilon_s}}, \tag{2}$$

The plasma frequency depends on some constant parameters such as static dielectric constant ε_s, reduced mass of electron and hole μ, and electronic charge *e*. Moreover, plasma frequency is an increasing function of carrier density N_{ext}, which is a changeable parameter. For bulk InAs, plasma frequency can be turned into THz band by adapting carrier density being larger than $10^{17}\ \mathrm{cm}^{-3}$, and hence, making plasma oscillation a tunable THz radiation source. Although sizes of layers in p-i-n diodes decrease to nanoscale, the material may remain its bulk properties. Thus, it may be expected to see similar coupling phenomenon in these structures.

The built-in electric field in InAs p-i-n diodes is found through Poisson's equation. However, Poisson's equation is only applied for homogeneous material [16c]. Therefore, to study dynamically interaction among plasmons and LO phonons, it is necessary to add one more term to the right-hand side of Poisson's equation as [9]

$$\nabla^2 \phi(\vec{r},t) = -4\pi \frac{\rho(\vec{r},t) + \rho_L(\vec{r},t)}{\varepsilon_\infty}, \tag{3}$$

where $\rho(\vec{r},t)$ is usual density of charge carriers and $\rho_L(\vec{r},t)$ is additional density of lattice polarization due to LO phonons, and ε_∞ is optical dielectric constant. The electric potential is found by solving Eq. (3) using finite difference method [28]. The transient built-in electric field at a grid point *n* and at a time *t* is determined through two neighboring electric potentials as

$$E_n(t) = \frac{\phi_n(t) - \phi_{n+1}(t)}{\Delta x}, \tag{4}$$

where Δx is distance between two grid points.

3. RESULTS AND DISCUSSION

Firstly, simulation parameters are introduced. Zero bias is then applied to consider effect of plasmon-polar phonon interaction on built-in electric field, which results mainly from photoexcited carriers. Photoexcited carriers are distributed randomly in diode according to Beer's law. The carrier density, N_{ext}, is taken from 0.5×10^{17} to $4.5\times10^{17}\ \mathrm{cm}^{-3}$, which satisfies coupling condition. The doping densities are $N_A = 1.0\times10^{17}\ \mathrm{cm}^{-3}$ and $N_D = 1.0\times10^{17}\ \mathrm{cm}^{-3}$. The thicknesses of the doping layers and the intrinsic layer are $d_p = d_n = 11\,\mathrm{nm}$ and $d_i = 410\,\mathrm{nm}$, respectively. The effective masses of electron and hole in Γ, L and X valleys are $m^*_{\Gamma e} = 0.023\ m_0$, $m^*_{\Gamma h} = 0.41\ m_0$,

$m_{Le}^{*} = 0.29\ m_0$, $m_{Xe}^{*} = 0.64\ m_0$, with m_0 being the bare mass of an electron. The bandgap is $E_{gap}^{\Gamma} = 0.354\,\text{eV}$, and the distance among Γ and L valleys is $\Delta E_{\Gamma L} = 0.73\,\text{eV}$ and among Γ and X valleys is $\Delta E_{\Gamma X} = 1.02\,\text{eV}$ [11, 12, 29]. The photocarriers are assumed to be excited by a laser beam with photon energy of 0.5 eV, which is larger than the above material bandgap [9]. The static and high-frequency dielectric constants of InAs are $\varepsilon_s = 15.15$ and $\varepsilon_\infty = 12.3$. The frequencies of LO and TO phonons are ω_{LO} = 7.01 THz and ω_{TO} = 6.44 THz [30]. The time and space are discretized into infinitesimal intervals of 0.20 fs and 8 Å, respectively.

Calculations are performed as follows. The intrinsic and doped carriers are injected and then are simulated until they get stable states. Then the photocarriers are excited in the diodes. The dynamics of all carriers, which forms built-in electric field, is simulated by the adapted Monte-Carlo method [17, 16a, 31]. The built-in electric field is monitored at the middle of *i*-layer for most stable data due to its longest distance to interfaces. The built-in electric field and its Fourier spectra are then drawn to investigate plasmon-polar phonon coupling interaction. With small time step and fine space grid as well as good Fourier transform tool, calculations may show clearly the effect of interaction. Calculation results are presented in Figs. 2-7 below.

It is hypothesized that plasmon-polar phonon coupling interaction significantly affects built-in electric field. Therefore, coupled modes are studied through the effect of coupling interaction on built-in electric field. It is expected that coupling interaction in InAs p-i-n diodes occurs when frequencies of LO phonons and plasmons are close to each other. In bulk InAs, plasma frequency is close to frequency of LO phonons, 7.01 THz [30], when density of carriers reaches $2 \times 10^{17}\ \text{cm}^{-3}$. In search of coupling interaction in range of the above density, Fourier transform of transient built-in electric field in the case without interaction is drawn (Fig. 2). The frequency spectrum is then drawn with a photocarrier density of $N_{ext} = 2 \times 10^{17}\ \text{cm}^{-3}$ at which there exists a bulk plasma oscillation with frequency of ~7 THz (marked by a two-headed arrow in Fig. 2). There are many peaks in frequency spectrum. The biggest peak, which overlaps bulk plasma peak, is attributed to main device plasma peak. The majority of particles in device are photocarriers; therefore, main device plasma oscillation is proposed to mostly come from photocarriers. There are also lower peaks, which are treated as fluctuations to main device plasma peak. The origin of these small peaks is explained in later discussion.

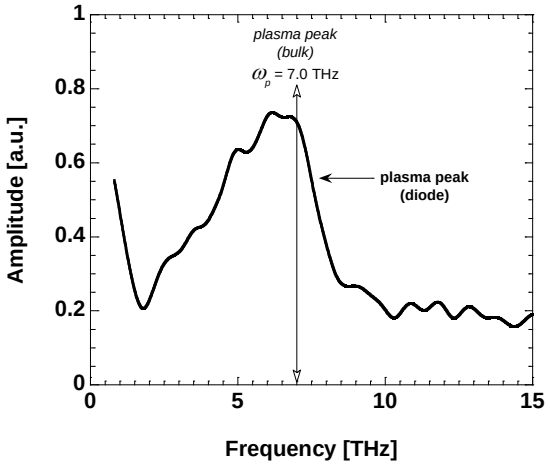

Fig. 2. Fourier transform spectrum of built-in electric field without plasmon-polar phonon interaction with carrier density of 2×10^{17} cm^{-3}.

To compare with results obtained in Fig. 2, frequency spectrum of transient built-in electric field in presence of plasmon-polar phonon coupling interaction is shown in Fig. 3. Positions of bulk plasmon-polar phonon coupled modes, L_+ (bulk) and L_- (bulk), are also pointed out for a comparison purpose. From Figs. 2 and 3, it can be seen that frequency spectra of transient built-in electric field in InAs p-i-n diodes are transformed significantly when coupling interaction is taken into account. Opposite to the non-coupling case, in which a wide plasma peak is observed (Fig. 2), a double-peak phenomenon is seen (Fig. 3). There appear two big peaks in spectrum, which deviate to the left from bulk counterparts. These peaks are credited to be coupled modes of device due to coupling interaction. A peak, namely peak L_+ (diode), stays in the band of proposed plasma peak in p-i-n diode (see Fig. 2). Besides, there is another peak, peak L_- (diode), which could not be seen in Fig. 2; however, it develops sharply in Fig. 3.

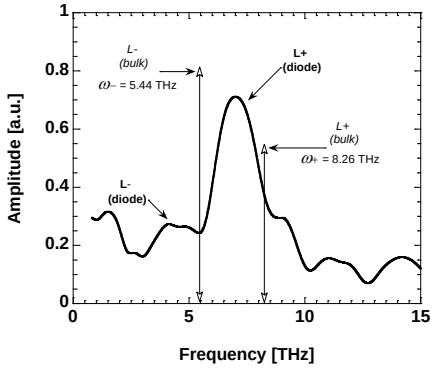

Fig. 3. Fourier transform of built-in electric field in presence of plasmon-polar phonon interaction with carrier density of 2×10^{17} cm^{-3}.

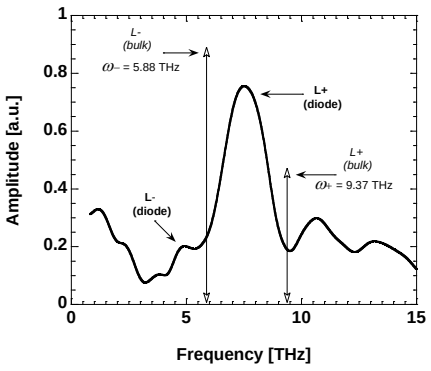

Fig. 4. Fourier transform of built-in electric field in presence of plasmon-polar phonon interaction with carrier density of 3×10^{17} cm^{-3}.

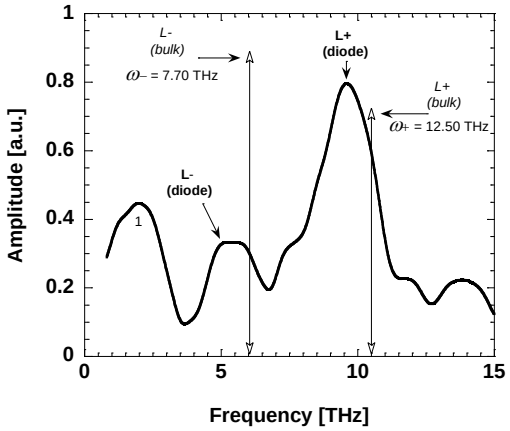

Fig. 5. Fourier transform of built-in electric field in presence of plasmon-polar phonon interaction with carrier density of 4×10^{17} cm^{-3}.

To definitely confirm the origin of the double-peak phenomenon above, other cases of carrier density, $N_{ext} = 3 \times 10^{17}$ cm^{-3} and $N_{ext} = 4 \times 10^{17}$ cm^{-3}, are considered as seen in Fig. 4 and Fig. 5. These density values deviate from 2×10^{17} cm^{-3}, i.e., the specific density suitable for occurrence of double-peak phenomenon under coupling interaction. In these cases, coupling interaction is proposed to weaken because coupling condition is just partly satisfied. That fact leads to a gradual decrease of double-peak phenomenon and peak L_{-} (diode) is gradually fuzzy. In both cases, two major peaks are observed but their positions are all shifted to the right compared to peak positions in Fig. 3, and peak L_{-} (diode) is lowered as proposed above. Moreover, the dependence of peak positions on carrier density in Figs. 3, 4 and 5 looks like bulk coupling dispersion relations. It is genuinely interesting if device dispersion relations look like bulk counterparts because it further supports our hypothesis that the two largest peaks are coupled modes in diode. To check that assumption, center positions of device peaks versus corresponding carrier density, which can be treated as device dispersion relations, are drawn, as seen in Fig. 6 (dashed lines). Besides, bulk coupling dispersion relations (solid lines) are also drawn for a comparison purpose. It is seen that device dispersion relations and bulk counterparts almost obey the same rules. These results support our hypothesis that the origin of the above double-peak phenomenon is plasmon-polar phonon coupling interaction.

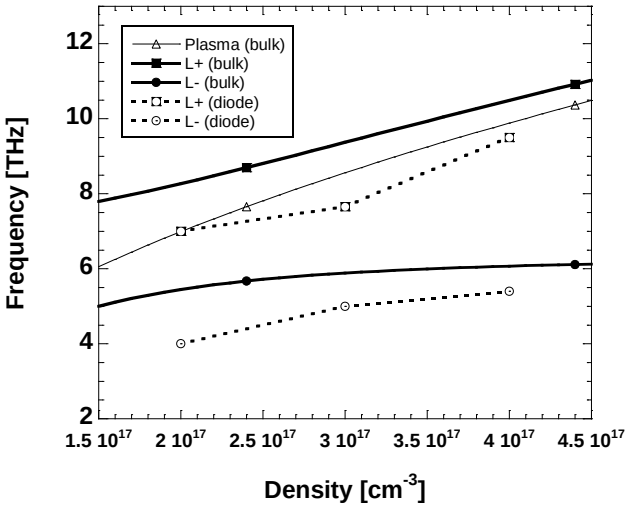

Fig. 6. Coupling dispersion relations in two cases: InAs p-i-n diode (dashed lines), and bulk InAs (solid lines).

In Figs. 3, 4 and 5 all other peaks with smaller amplitudes are seen. They seem to repeat from one peak at a certain repeating rate. The repeating can be seen clearest in Fig. 5. Suppose peak No. 1 in Fig. 5 is also a plasma peak in diode but originating from doped carriers of *p* and *n*-layers, the doped carriers exist in diode before photocarriers are excited, and doped carriers are accompanied by their own plasma oscillation, namely, doped plasma. When there are photocarriers, there also exists their own plasma oscillation, namely, main device plasma. Both these plasmas of doped carriers and photocarriers oscillate independently for a long time until they merge into a combined oscillation due to drift movement of carriers under built-in electric field. Therefore, if electric field is measured in the femtosecond time scale as in this case, superposition signal of those two plasma oscillations can be seen. Consequently, in frequency spectrum of the electric field, two separate plasma peaks will be seen. Moreover, other small peaks appear to be replicas of peak No. 1 at a certain repeating rate. In other words, their frequencies seem to be results of multiplication of an integer with frequency of peak No. 1. It is proposed that this phenomenon is consequence of peak clipping by diode [27b]. If a larger frequency range is considered, more repeated peaks can be seen. In this case, diode works as a high-order harmonic generator [32].

In our previous work, plasmon-polar phonon coupled modes in GaAs p-i-n diodes have been studied [9]. Double-mode phenomenon in frequency spectrum of built-in electric field has been found when plasmon-polar phonon interaction is taken into account. However, spectra in GaAs and InAs p-i-n diodes are different from each other. Peaks observed in InAs p-i-n diodes are broader than ones archived in GaAs counterparts. The reason is related to effective masses of electrons and holes in devices [9]. In addition, in this study of InAs p-i-n diodes, bulk-like dispersion relations of

coupled modes, which have not been archived in GaAs p-i-n diodes before due to limit of calculation, are found. Furthermore, an interesting phenomenon related to mode clipping (Figs. 3, 4 and 5), which has not been observed in GaAs p-i-n diodes before, are noticed.

4. CONCLUSION

So far, characteristics of plasmon-polar phonon coupled modes in InAs p-i-n diodes have been studied. To reveal the role of coupled modes, built-in electric field is calculated in both cases, with, and without, plasmon-polar phonon interaction. Double-peak phenomenon in frequency spectrum of built-in electric field with coupling interaction was observed. In addition, those two peaks lie in THz range and deviate from two coupled modes of InAs bulk semiconductor. Moreover, bulk-like dispersion relations of plasmon-polar phonon coupled modes of diode were found. These results support our assumption that the origin of double-peak phenomenon is plasmon-polar phonon coupling interaction. In other words, these results reveal the significance of coupled modes. Therefore, coupling interaction should be considered in the cases in which there are suitable conditions for the existence of coupling phenomena. Finally, replicas of small peaks due to peak clipping by diode was found, which is an interesting phenomenon that could not be seen in bulk semiconductor.

REFERENCES

[1]. A. Y. Pawar, D. D. Sonawane, K. B. Erande, and D. V. Derle (2013). Terahertz technology and its applications. *Drug Invention Today*, 5, pp. 157-163.

[2]. A. U. Sokolnikov (2013). "Medical and Other Applications of THz Radiation. THz Identification for Defense and Security Purposes", World Scientific, Singapore, 1st ed., Chap. 8, pp. 193-216.

[3]. R. A. Lewis (2014). A review of terahertz sources. *J. Phys. D: Appl. Phys.*, 47, pp. 374001 (1-11).

[4]. V. Apostolopoulos, and M. E. Barnes (2014). THz emitters based on the photo-Dember effect, *J. Phys. D: Appl. Phys.*, 47, pp. 374002 (1-16).

[5]. M. Mittendorff, M. Xu, R. J. B. Dietz, H. Kunzel, B. Sartorius, H. Schneider, M. Helm and S. Winnerl (2013). Terahertz generation and detection with InGaAs-based large-area photoconductive devices excited at 1.55m. *Nanotechnology*, 24, pp. 214007 (1-4).

[6]. V. Ryzhii, I. Khmyrova, M. Ryzhii, A. Satou, T. Otsuji, V.Mitin, and M. S. Shur (2007). *Int. J. High Speed Electron. Syst.*, 17, pp. 521-538.

[7]. A. Reklaitis (2006). Erratum: Monte Carlo analysis of terahertz oscillations of photoexcited carriers in GaAs p-i-n structures. *Phys. Rev. B*, 74, pp. 165305 (1-9).

[8]. A. Leitenstorfer, S. Hunsche, J. Shah, M. C. Nuss, and W. H. Knox (2000). Femtosecond high-field transport in compound semiconductors. *Phys. Rev. B*, 61, pp. 16642-16652.

[9]. D. N. Thao, and N. P. The (2013). Effect of Longitudinal Optical Phonon–Plasmon Coupling on the Transient Self-Consistent Field in GaAs p–i–n Diodes. *J. Phys. Soc. Jpn.*, 82, pp. 104701 (1-4).

[10]. M. Born, and K. Huang (1998). "Dynamical Theory of Crystal Lattices". Oxford University Press, London, 4th ed., Chap. 2, p. 94.

[11]. M. Cardona (1961). Electron effective masses of InAs and GaAs as a function of temperature and doping M. Cardona. *Phys. Rev.*, 121, pp. 752-758.

[12]. N. Bouarissa, and H. Aourag (1999). Effective masses of electrons and heavy holes in InAs, InSb, GaSb, GaAs and some of their ternary compounds. Infrared Physics & Technology, 40, pp. 343-349.

[13]. N. Sarukura, H. Ohtake, S. Lzumida, and Z. Liu (1998). High average-power THz radiation from femtosecond laser-irradiated InAs in a magnetic field and its elliptical polarization characteristics. *J. App. Phys.*, 84, pp. 654-656.

[14]. S. Datta (2000). Nanoscale device modeling: the Green's function method. *Superlattices Microstruct.*, 28, pp. 253-278.

[15]. J. Even, L. Pedesseau, E. Tea, S. Almosni, A. Rolland, C. Robert, J. Jancu, C. Cornet, C. Katan, J. Guillemoles, and O. Durand (2014). Density Functional Theory Simulations of Semiconductors for Photovoltaic Applications: Hybrid Organic-Inorganic Perovskites and III/V Heterostructures. Int. J. Photoenergy, 2014, pp. 649408 (1-11).

[16]. K. Tomizawa (1993). "Numerical simulation of submicron semiconductor devices". Artech House, Boston·London, 1st ed., a) Chap. 4, p. 115. b) Chap. 2, p. 56. c) Chap. 2, p. 58.

[17]. D. N. Thao, S. Katayama, T. D. Khoa, and M. Iida (2004). Calculation of THz radiation due to coherent polar-phonon oscillations in p–i–n diode structure at high electric field. *Semicond. Sci. Technol.*, 19, pp. S304-S307.

[18]. M. Abe, S. Madhavi, Y. Shimada, Y. Otsuka, K. Hirakawa, and K. Tomizawa (2002). Transient carrier velocities in bulk GaAs: Quantitative comparison between terahertz data and ensemble Monte Carlo calculations. *Appl. Phys. Lett.*, 81, pp. 679-681.

[19]. D. N. Thao, S. Katayama, and K. Tomizawa (2004). Numerical simulation of THz radiation by coherent LO phonons in GaAs p–i–n diodes under high electric fields. *J. Phys. Soc. Jpn.*, 73, pp. 3177-3181.

[20]. H. Kosina and M. Nedjalkov (2003). Particle Models for Device Simulation. *Int. J. Hi. Spe. Ele. Syst.*, 13, pp. 727-769.

[21]. C. Jacoboni and L. Reggiani (1983). The Monte Carlo method for the solution of charge transport in semiconductors with applications to covalent materials. *Rev. Mod. Phys*., 55, pp. 645-705.

[22]. M. B. Johnston, D. M. Whittaker, A. Corchia, A. G. Davies, and E. H. Linfield (2002). Simulation of terahertz generation at semiconductor surfaces. Phys. Rev. B, 65, pp. 165301 (1-8).

[23]. M. B. Johnston, A. Dowd, R. Driver, E. H. Linfield, A. G.. Davies, and D. M. Whittaker (2004). Emission of collimated THz pulses from photo-excited semiconductors. *Semicond. Sci. Technol.*, 19, S449-S451.

[24]. J. Lloyd-Hughes, S. K. E. Merchant, L. Sirbu, I. M. Tiginyanu, and M. B. Johnston (2008). Terahertz photoconductivity of mobile electrons in nanoporous InP honeycombs. *Phys. Rev. B*, 78, pp. 085320 (1-4).

[25]. M. Saraniti, Y. Hu, S. M. Goodnick, and S. J. Wigger (2002). Overshoot velocity in ultra-broadband THz studies in GaAs and InP. *Physica B*, 314, pp. 162-165.

[26]. J. Shah (Ed.) (1992). "Hot Carriers in Semiconductor Nanostructures: Physics and Applications". Academic Press, Inc, New York, 1st ed., Vol. 8, Chap. 3, p. 191.

[17]. S. W. Smith (1999). "The Scientist and Engineer's Guide to Digital Signal Processing". California Technical Publishing, San Diego, California, 2nd ed. , a) Chap. 15, p. 278 and Chap. 16, p. 286. b) Chap. 13, p. 260.

[28]. J. D. Hoffman (2001). "Numerical Methods for Engineers and Scientists". CRC Press, London, 2nd ed., Chap. 9, p. 555.

[29]. Z. M. Fang, K. Y. Ma, D. H. Jaw, R. M. Cohen, and G. B. Stringfellow (1990). Photoluminescence of InSb, InAs, and InAsSb grown by organometallic vapor phase epitaxy**.** *J. Appl. Phys.*, 67, pp. 7034-7039.

[30]. D.J. Lockwood, G. Yu, and N.L. Rowell (2005). Optical phonon frequencies and damping in AlAs, GaP, GaAs, InP, InAs and InSb studied by oblique incidence infrared spectroscopy. Solid State Commun., 136, pp. 404-409.

[31]. D. N. Thao, S. Katayama, and K. Tomizawa (2004). Numerical Simulation of THz Radiation by Coherent LO Phonons in GaAs p–i–n Diodes under High Electric Fields. *J. Phys. Soc. Jpn*., 73, pp. 3177-3181.

[32]. S. Banerjee, A. R. Valenzuela, R. C. Shah, A. Maksimchuk, and D. Umstadter (2003), High-harmonic generation in plasmas from relativistic laser-electron scattering. *J. Opt. Soc. Am. B*, 20, pp. 182-190.

CÁC MODE KẾT CẶP PLASMON – PHONON PHÂN CỰC TRONG CẤU TRÚC ĐI-ỐT InAs

Lê Thị Ngọc Bảo[1], Lê Thị Diệu Hiền[1], Đinh Như Thảo[2]*

[1]Trường Đại học Khoa học, Đại học Huế

[2]Trường Đại học Sư phạm, Đại học Huế

*Email: dnthao@hueuni.edu.vn; ltnbao@husc.edu.vn

TÓM TẮT

Bài báo trình bày các kết quả mô phỏng số về đặc trưng của các mode kết cặp plasmon–phonon phân cực trong cấu trúc đi-ốt InAs dạng p–i–n. Khi xét đến tương tác plasmon–phonon phân cực, hiện tượng chồng chập của hai mode mới trong phổ tần số của điện trường bên trong được quan sát. Ngoài ra, sự phụ thuộc tần số của các mode vào mật độ hạt tải cho thấy có sự tương đồng với hệ thức tán sắc của các mode kết cặp plasmon–phonon phân cực trong vật liệu khối. Do đó, hai mode mới này có thể được xác định là các mode kết cặp plasmon–phonon phân cực trong cấu trúc đi-ốt. Hơn nữa, một dải mode có biên độ nhỏ xuất hiện do hiệu ứng cắt biên bởi cấu trúc đi-ốt cũng đã được tìm thấy.

Từ khoá: InAs; cấu trúc đi-ốt p–i–n; tương tác plasmon–phonon phân cực; mode kết cặp; tần số terahertz.

Đinh Như Thảo sinh ngày 17/02/1975 tại Hải Dương. Năm 1997, ông tốt nghiệp Cử nhân khoa học ngành Vật lý tại Trường Đại học Khoa học, Đại học Huế. Năm 1999, ông tốt nghiệp Thạc sĩ chuyên ngành Vật lý lý thuyết và Vật lý toán tại Viện Vật lý, Viện Hàn lâm Khoa học và Công nghệ Việt Nam. Năm 2004, ông tốt nghiệp Tiến sĩ chuyên ngành Khoa học vật liệu tại Viện Khoa học và Công nghệ Tiên tiến Nhật Bản (JAIST). Năm 2013, ông được bổ nhiệm chức danh PGS. Từ năm 2005 đến nay ông giảng dạy tại Trường Đại học Sư phạm, Đại học Huế.

Lĩnh vực nghiên cứu: Vật lý lý thuyết và vật lý toán.

Lê Thị Ngọc Bảo sinh ngày 31/10/1983 tại thành phố Huế. Năm 2006, bà tốt nghiệp Cử nhân khoa học ngành Vật lý tại Trường Đại học Khoa học, Đại học Huế. Năm 2009, bà tốt nghiệp Thạc sĩ chuyên ngành Vật lý lý thuyết và Vật lý toán tại trường Đại học Sư phạm, Đại học Huế. Năm 2020, nhận bằng Tiến sĩ chuyên ngành Vật lý lý thuyết và Vật lý toán tại Trường Đại học Sư phạm, Đại học Huế. Từ năm 2006 đến nay, bà là giảng viên của Khoa Vật lý, nay là Khoa Điện, Điện tử và Công nghệ vật liệu, Trường Đại học Khoa học, Đại học Huế.

Lĩnh vực nghiên cứu: Vật lý lý thuyết và vật lý toán.

Lê Thị Diệu Hiền sinh ngày 03/02/1989 tại thành phố Huế. Năm 2011, bà tốt nghiệp cử nhân ngành Vật lý Tiên tiến tại Trường Đại học Sư phạm, Đại học Huế. Năm 2013, bà tốt nghiệp thạc sĩ chuyên ngành Vật lý lý thuyết và vật lý toán tại trường Đại học Sư phạm, Đại học Huế. Năm 2023 tốt nghiệp Tiến sĩ chuyên ngành Vật lý lý thuyết và Vật lý toán tại trường Đại học Sư phạm, Đại học Huế. Bà giảng dạy tại trường Đại học Khoa học, Đại học Huế.

Lĩnh vực nghiên cứu: Vật liệu có cấu trúc nano, mô phỏng lý thuyết.